

Direct Observation of Polarization Mixing in Nuclear Bragg X-Ray Scattering of Synchrotron Radiation

D. P. Siddons, J. B. Hastings, G. Faigel,^(a) L. E. Berman, P. E. Haustein, and J. R. Grover

Brookhaven National Laboratory, Upton, New York 11973

(Received 3 January 1989)

The direct observation of a polarization mixing in nuclear Bragg scattering of synchrotron radiation by α -⁵⁷Fe₂O₃ is reported. Application of a magnetic bias field having the appropriate orientation was shown to produce almost complete rotation of the σ -polarized incident beam to a π -polarized diffracted beam. Rotation of this field about the diffraction vector through 90° caused the diffracted beam polarization to change continuously from σ through elliptical to π , as predicted theoretically.

PACS numbers: 76.80.+y, 24.70.+s, 29.75.+x

The study of nuclear Bragg scattering (NBS) has benefitted significantly from the use of synchrotron radiation (SR) as a photon source. In previous experiments, the pulsed nature of SR has permitted detailed investigations of the time dependence of the scattered beam from yttrium iron garnet¹ (a ferrimagnet) and the simple antiferromagnets FeBO₃² and α -Fe₂O₃.^{3,4} The theory of nuclear Bragg scattering⁵ has not only addressed the time evolution of the scattered radiation, but also the polarization dependence of the scattered beam as a function of both the incident beam polarization and the orientation of the nuclear quantization axis with respect to the scattering plane. Experimental investigations of these polarization phenomena are the subject of this Letter.

⁵⁷Fe has a strong Mössbauer resonance at 14.413 keV. This resonance is a degenerate multiplet with a components corresponding to changes in the magnetic quantum number m . Allowed changes include $\Delta m = 0$ and ± 1 . The $\Delta m = 0$ transitions correspond to linear oscillators, whereas the $\Delta m = \pm 1$ transitions correspond to circular oscillators whose chirality depends on the sign of Δm . In the presence of local fields and field gradients such as those found in crystals, the degeneracy is removed and a fine structure can be resolved. The magnetic structure of α -⁵⁷Fe₂O₃ is an antiferromagnetic arrangement of ferromagnetic sheets stacked in the (*hhh*)

direction (rhombohedral indices).⁶ The spins lie in the (*hhh*) planes but are not quite antiparallel layer to layer yielding a small, in-plane, ferromagnetic moment. It is this moment that couples to an applied external field and allows the alignment of the quantization axis with respect to the scattering plane.

The existence of pure nuclear Bragg reflections from α -⁵⁷Fe₂O₃ has previously been demonstrated using a ⁵⁷Co radioactive source.⁷ Measurements of the influence of magnetic field orientation on the spectrum of unpolarized γ rays diffracted by the same sample have also been performed.⁸ More recently a pure nuclear Bragg reflection has been observed using SR.^{3,4} In this work we have also used synchrotron radiation, and we have further taken advantage of its high degree of linear polarization to measure the polarization properties of the nuclear scattering.

Among the predictions for scattering by circular oscillators is that of polarization mixing⁵ in which the polarization state of polarized incident beam may be modified on Bragg reflection depending on the orientations of the nuclear oscillators relative to the scattering plane. The present work was undertaken to study these predictions experimentally. The polarization dependence of nuclear Bragg scattering is contained in the structure factor for photons near a nuclear resonance. Following van B urck *et al.*⁹ this may be written as

$$g_{ji}^{(l)}(E) = -\frac{3}{2} \frac{\lambda^2}{\pi V} \sum_{\rho} \frac{1}{k_{\text{vac}}} \frac{1}{2I_g + 1} \frac{\eta}{1 + \alpha} \frac{(E - E_{0l})^{\frac{1}{2}} \Gamma - i(\frac{1}{2} \Gamma)^2}{(E - E_{0l})^2 + \frac{1}{2} \Gamma^2} \times C_l^2(I_g, 1, I_e; m_{gl}, \Delta m_l) f_{\rho}(\mathbf{k}_j) f_{\rho}(\mathbf{k}_i) \exp[i(\mathbf{k}_j - \mathbf{k}_i) \cdot \mathbf{r}_{\rho}] P_{ji}^{n(l)}. \quad (1)$$

In the above equation the sum is over the resonant atoms in the unit cell. E is the incident photon energy, λ is the wavelength, V is the unit-cell volume, and k_{vac} is the incident wave vector. I_g is the spin of the ground state, η is the abundance of the resonant nuclei, and α is the conversion coefficient. E_{0l} denotes the energy of l th multiplet level and Γ its total width. $f_{\rho}(\mathbf{k}_j)$ is the Lamb-M ossbauer factor, C_l the Clebsch-Gordan coefficient for a given transition from I_g to the excited state I_e , and Δm_l the corresponding change in the magnetic quantum number. The position of the resonant nucleus in the unit cell is denoted by \mathbf{r}_{ρ} . The incident and scattered directions are indicated by subscripts i and j , respectively. The element $P_{ji}^{n(l)}$ is the polarization factor describing the coupling of the transitions to the electromagnetic field, and can be written as

$$P_{ji}^{n(l)} = \begin{cases} (\hat{\mathbf{h}}_i \cdot \hat{\mathbf{u}}_z), (\hat{\mathbf{h}}_j \cdot \hat{\mathbf{u}}_z), & \Delta m = 0, \\ \frac{1}{2} \{ (\hat{\mathbf{h}}_i \cdot \hat{\mathbf{h}}_j) - h(\hat{\mathbf{h}}_i \cdot \hat{\mathbf{u}}_z)(\hat{\mathbf{h}}_j \cdot \hat{\mathbf{u}}_z) \pm i[(\hat{\mathbf{h}}_i \times \hat{\mathbf{h}}_j) \cdot \hat{\mathbf{u}}_z] \}, & \Delta m = \pm 1. \end{cases} \quad (2)$$

In Eq. (2), \hat{u}_z is the quantization axis unit vector (spin direction at the atom site) and \hat{h}_i and \hat{h}_j are the magnetic field unit vectors of the incident and diffracted beams. Since Fe_2O_3 is an antiferromagnetic, \hat{u}_z is reversed in alternate crystallographic layers. The polarization factor for one magnetic period is thus the sum of two expressions of the form (2), where $\hat{u}_z^A = -\hat{u}_z^B$. Finite contributions arise only for transitions having $\Delta m = \pm 1$, i.e., for four of the six hyperfine components. For each of two orthogonal quantization axis orientations, there are four possible combinations of the incident and diffracted beam linear polarizations and the net polarization factor for each case is shown in Table I. The electric polarization perpendicular and parallel to the diffraction plane will be designated as σ and π , respectively.

These predictions can be stated as follows: For \hat{u}_z perpendicular to the scattering plane, only the σ component of the incident beam is diffracted, and appears σ polarized in the diffracted beam. No polarization mixing occurs and the π -polarization state is completely suppressed. For \hat{u}_z parallel to the diffraction plane, the normal scattering, where the incident and diffracted beams have the same polarization, is completely suppressed. The only scattering which is observed is purely mixed, i.e., a σ -polarized incident beam produces a π -polarized diffracted beam and vice versa, as shown in Table I.

The sample used for the measurements was the same nearly perfect $\alpha\text{-}^{57}\text{Fe}_2\text{O}_3$ crystal used in our previous studies.^{3,4} The apparatus consisted of an improved version of our ultrahigh-resolution monochromator¹⁰ placed downstream of the standard two-crystal monochromator which is fed by the six-pole wiggler device installed in the Cornell High Energy Synchrotron Source (CHESS) facility at Cornell University. The storage ring operated at 5.29 GeV with a stored electron current of approximately 50 mA during these experiments. The sample was mounted on the Ω axis of a diffractometer (see Fig. 1). A Sm-Co permanent magnet with iron pole pieces was mounted on the ϕ axis such that the field direction could be rotated about the sample [1,1,1] direction (rhombohedral indices). The field was measured to be about 1 kG at the sample position. The x-ray beam diffracted by the sample was passed to a polarization analyzer and then to a solid-state detector. The polarization analyzer consisted of a nearly perfect single crys-

tal of beryllium metal.¹¹ For the (00.6) reflection (hexagonal indices) the Bragg angle for 14.413-keV photons is 46° . The Be crystal used in these measurements had a mosaic spread of approximately 40 arcsec, and gave a peak reflectivity of $> 20\%$ for the (00.6) reflection using Mo $K\alpha$ radiation (17.44 keV).

Consideration of the stability of the various components of the apparatus relative to their respective sensitivities led to the use of the following measurement scheme. The polarization analyzer was optimized by rocking through its Bragg reflection range and then setting it at its midpoint. Since its rocking curve is rather broad compared to the angular stability of its mount, its Bragg angle was not subsequently altered during the measurement. In contrast, the range of Bragg reflection for the sample was approximately 3 arcsec, of the same order as the stability of the diffractometer. Intensities were therefore measured by integrating over the sample rocking curve, rather than over the analyzer rocking curve as is more traditionally done. There is one difficulty with this scheme, and that arises when it is necessary to set the analyzer to the π setting. Then the relevant beam divergence for the analyzer crystal is the horizontal divergence. For the conditions used in these experiments, this was comparable to the analyzer mosaic spread. Thus the analyzer could not be relied upon to make an accurate integration over this beam divergence, as it could in the σ case. The result of this is that the measured intensities are not comparable across the σ and π analyzer settings. This is not a serious difficulty since absolute intensities for the two cases are never compared.

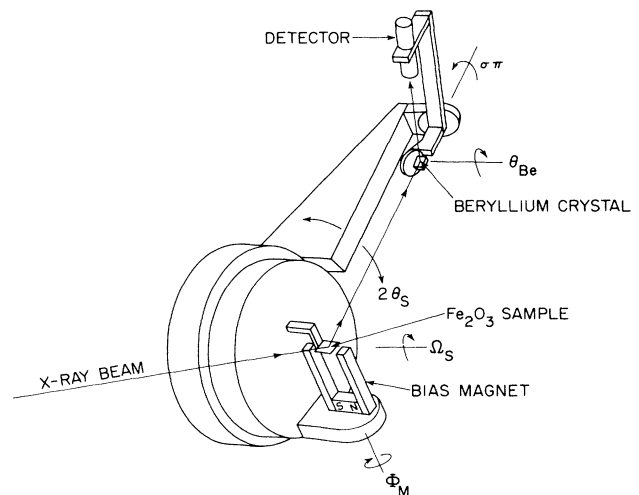


TABLE I. Summary of the polarization factors for the different beam polarizations and spin orientations.

Incident beam polarization h_i	Diffracted beam polarization h_j	Polarization factor $P_{ij}^{(0)}$	
		$\hat{u}_z \parallel$	$\hat{u}_z \perp$
σ	σ	0	$\sin 2\theta$
σ	π	$\cos \theta$	0
π	σ	$\cos \theta$	0
π	π	0	0

FIG. 1. A schematic view of the diffractometer which carries the sample and its polarizing magnet. The magnetic field direction can be rotated about the sample diffraction vector. Polarization analysis of the diffracted beam is done by the beryllium crystal and its detector. The scattering plane of the beryllium can be rotated about the diffracted beam from the sample.

TABLE II. Integrated intensities (arbitrary units) for the four possible combinations of the polarization analyzer setting and the spin orientations.

	$\hat{u}_z \perp$	$\hat{u}_z \parallel$
σ	840	85
π	5	455

Separate measurements were made with the analyzer set to transmit σ - and π -polarized radiation. At each setting, the magnetic quantization axis was changed from 0 to 90° in steps of 15°. More data were acquired at the extremal angles to give better statistics for the "pure" settings (i.e., those giving all σ or all π). Integrated data for these pure settings are given in Table II, and the rocking curves are shown in Fig. 2.

It is interesting to note that, in Fig. 2, the contrast between $\hat{u}_z \perp$ and $\hat{u}_z \parallel$ is much greater for the π setting of the analyzer than for the σ setting. In Fig. 2(a) the low-intensity data correspond to the polarization mixing case with the analyzer set to pass σ . Thus, the π -polarized component of the incident beam will be switched to σ in the diffracted beam, and hence will be detected. Of course, this π component of the incident synchrotron beam is much weaker than the σ component. Conversely, the low-intensity curve in Fig. 2(b) corresponds to the nonmixing case with the polarizer set to pass π . Since the theory predicts that in the nonmixing case π -polarized radiation does not couple to any of the transitions, no diffracted intensity is observed.

For intermediate directions of the magnetic quantization axis, the radiation should be elliptically polarized. Figure 3 shows data for such intermediate orientations of magnetic field. Data for σ and π polarization of the scattered beam are shown together, with arbitrary scales. The complementary behavior is readily apparent, despite the inability to directly compare the absolute σ and π intensities to each other. These data are consistent with a continuous transition from σ through elliptical to π polarization. A full determination of the polarization state requires the use of a filter which passes only circularly polarized light. However, the data presented above represent persuasive evidence that the observed polarization behavior of nuclear Bragg scattering agrees with the theoretical predictions.

In summary, we have made direct observations of polarization mixing phenomena in the nuclear Bragg scattered synchrotron radiation from α -hematite using a Bragg reflection polarization analyzer. The rotation of the polarization plane of the diffracted radiation from σ to π in the mixing geometry is shown to be complete within the limits of observation. Further, it is found that scattering of π -polarized radiation in the nonmixing geometry is forbidden. The observed effects are in ac-

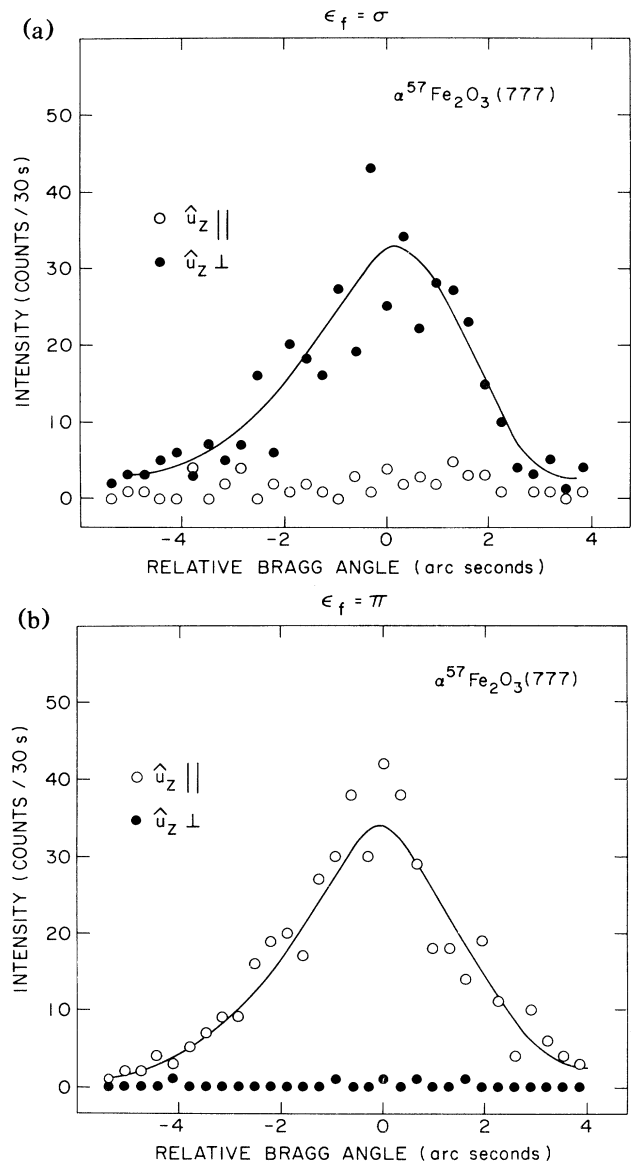


FIG. 2. (a) Rocking curves at resonance for orientations of the magnetic quantization axis parallel and perpendicular to the scattering plane, with the polarization analyzer set to transmit σ -polarized radiation. As predicted, the intensity is greater for \hat{u}_z perpendicular to the diffraction plane. (b) As in (a), but for the case when the polarization analyzer is set to transmit π -polarized radiation. Note that the signal for \hat{u}_z perpendicular to the diffraction plane is much less than that for \hat{u}_z parallel in (a).

cord with theoretical predictions. In addition, we point out that it is now possible to generate an x-ray beam having very long coherence lengths with switchable polarization orientation. Such a beam should have interesting applications in fundamental optics and polarization-dependent inelastic x-ray scattering experiments.

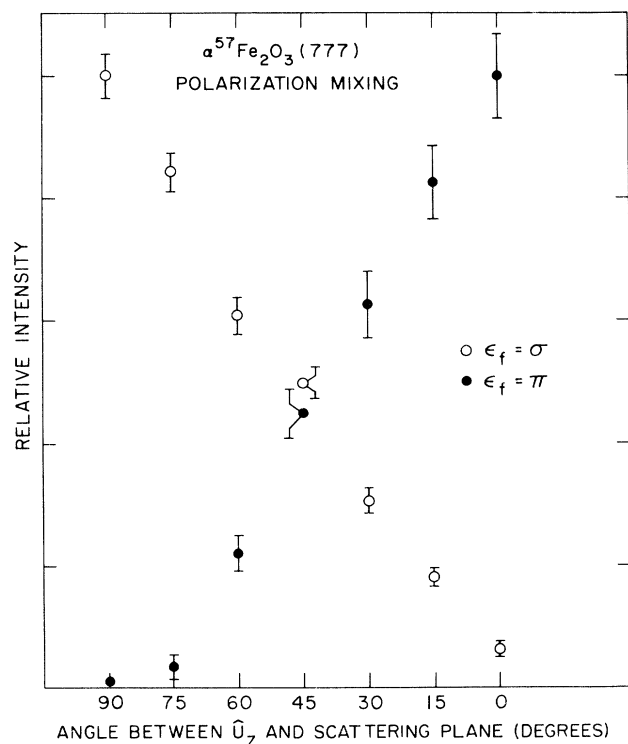


FIG. 3. Intensity scattered into the σ - and π -polarization directions as a function of the orientation of the magnetic quantization axis.

We are extremely grateful to Dr. A. K. Freund of the European Synchrotron Radiation Facility for the loan of the beryllium single crystal which was grown by Sibylle Stiltz of Max-Planck-Institute in Stuttgart, West Germany, and to J. P. Remeika and A. S. Cooper of AT&T

Bell Labs who grew the hematite crystal. We are also indebted to Professor B. W. Batterman and the staff of the CHESS facility at Cornell University for their generous cooperation in these endeavors. This work was performed under the auspices of the Department of Energy, Contract No. DE-AC02-76CH00016.

(a)Present address: Central Research Institute of Physics, Budapest, Hungary.

¹E. Gerdau, R. Ruffer, H. Winkler, W. Tolksdorf, C. P. Klager, and J. P. Hannon, *Phys. Rev. Lett.* **54**, 835 (1985).

²U. van Bürck, R. L. Mössbauer, E. Gerdau, R. Ruffer, R. Hollatz, G. V. Smirnov, and J. P. Hannon, *Phys. Rev. Lett.* **59**, 355 (1987).

³G. Faigel, D. P. Siddons, J. B. Hastings, P. E. Haustein, J. R. Grover, J. P. Remeika, and A. S. Cooper, *Phys. Rev. Lett.* **58**, 2699 (1987).

⁴G. Faigel, D. P. Siddons, J. B. Hastings, P. E. Haustein, J. R. Grover, and L. E. Berman, *Phys. Rev. Lett.* **61**, 2794 (1988).

⁵See, for example, J. P. Hannon and G. T. Trammell, *Phys. Rev.* **186**, 306 (1969); Yu Kagan and A. M. Afanas'ev, *Z. Naturforsch.* **28a**, 1351 (1973), and references therein.

⁶C. G. Shull, W. A. Strauss, and E. P. Wollan, *Phys. Rev.* **83**, 333 (1951).

⁷G. V. Smirnov, V. V. Sklyarevskii, R. A. Voskanyan, and A. N. Artem'ev, *Pis'ma Zh. Eksp. Teor. Fiz.* **9**, 123 (1969) [*JETP Lett.* **9**, 70 (1969)].

⁸A. N. Artem'ev, V. V. Sklyarevskii, G. V. Smirnov, and E. P. Stepanov, *Pis'ma Zh. Eksp. Teor. Fiz.* **15**, 320 (1972) [*JETP Lett.* **15**, 226 (1972)].

⁹U. van Bürck, G. V. Smirnov, R. L. Mössbauer, F. Parak, and N. A. Semioschkina, *J. Phys. C* **11**, 2305 (1978).

¹⁰D. P. Siddons, J. B. Hastings, and G. Faigel, *Nucl. Instrum. Methods, Phys. Rev., Sect. A* **266**, 329 (1988).

¹¹S. Stiltz and A. Freund, *J. Cryst. Growth* **88**, 321 (1988).